



**HAL**  
open science

## Enhancing Cycling Stability and Specific Capacitance of Vanadium Nitride Electrodes by Tuning Electrolyte Composition

Emile Haye, Yuanyuan Miao, David Pilloud, Camille Douard, Rabah Boukherroub, Jean-François Pierson, Thierry Brousse, Stéphane Lucas, Laurent Houssiau, Jean-Jacques Pireaux, et al.

### ► To cite this version:

Emile Haye, Yuanyuan Miao, David Pilloud, Camille Douard, Rabah Boukherroub, et al.. Enhancing Cycling Stability and Specific Capacitance of Vanadium Nitride Electrodes by Tuning Electrolyte Composition. *Journal of The Electrochemical Society*, 2022, 169 (6), 063503, 8 p. 10.1149/1945-7111/ac7353 . hal-03682462

**HAL Id: hal-03682462**

**<https://hal.science/hal-03682462>**

Submitted on 31 May 2022

**HAL** is a multi-disciplinary open access archive for the deposit and dissemination of scientific research documents, whether they are published or not. The documents may come from teaching and research institutions in France or abroad, or from public or private research centers.

L'archive ouverte pluridisciplinaire **HAL**, est destinée au dépôt et à la diffusion de documents scientifiques de niveau recherche, publiés ou non, émanant des établissements d'enseignement et de recherche français ou étrangers, des laboratoires publics ou privés.



Distributed under a Creative Commons Attribution - NonCommercial - NoDerivatives 4.0 International License

ACCEPTED MANUSCRIPT

## Enhancing Cycling Stability and Specific Capacitance of Vanadium Nitride Electrodes by Tuning Electrolyte Composition

To cite this article before publication: Emile HAYE *et al* 2022 *J. Electrochem. Soc.* in press <https://doi.org/10.1149/1945-7111/ac7353>

### Manuscript version: Accepted Manuscript

Accepted Manuscript is “the version of the article accepted for publication including all changes made as a result of the peer review process, and which may also include the addition to the article by IOP Publishing of a header, an article ID, a cover sheet and/or an ‘Accepted Manuscript’ watermark, but excluding any other editing, typesetting or other changes made by IOP Publishing and/or its licensors”

This Accepted Manuscript is © 2022 The Author(s). Published by IOP Publishing Ltd..

This article can be copied and redistributed on non commercial subject and institutional repositories.

Although reasonable endeavours have been taken to obtain all necessary permissions from third parties to include their copyrighted content within this article, their full citation and copyright line may not be present in this Accepted Manuscript version. Before using any content from this article, please refer to the Version of Record on IOPscience once published for full citation and copyright details, as permissions will likely be required. All third party content is fully copyright protected, unless specifically stated otherwise in the figure caption in the Version of Record.

View the [article online](#) for updates and enhancements.

## Enhancing Cycling Stability and Specific Capacitance of Vanadium Nitride Electrodes by Tuning Electrolyte Composition

Journal:	<i>Journal of The Electrochemical Society</i>
Manuscript ID	JES-107194.R1
Manuscript Type:	Research Paper
Date Submitted by the Author:	03-May-2022
Complete List of Authors:	HAYE, Emile; UNamur, MIAO, Yuanyuan; IEMN PILLOUD, David; Institut Jean Lamour Douard, Camille; Université de Nantes, CNRS, Institut des Matériaux Jean Rouxel, IMN, F-44000 Nantes, France Boukherroub, Rabah ; Interdisciplinary Research Institute (IRI) Pierson, Jean-Francois; Université de Lorraine Brousse, Thierry; Institut des Matériaux Jean Rouxel (IMN) University of Nantes/CNRS, Polytech Nantes LUCAS, Stéphane; UNamur HOUSSIAU, Laurent; UNamur PIREAUX, Jean-Jacques; UNamur ACHOUR, Amine; UNamur
Keywords:	Vanadium nitride, Thin film electrode, Cycling stability, Pseudocapacitance

SCHOLARONE™  
Manuscripts

# Enhancing Cycling Stability and Specific Capacitance of Vanadium Nitride Electrodes by Tuning Electrolyte Composition

Emile Haye,<sup>1,z</sup> Yuanyuan Miao,<sup>2</sup> David Pilloud,<sup>3</sup> Camille Douard,<sup>4,5</sup> Rabah Boukherroub,<sup>2</sup> Jean-François Pierson,<sup>3</sup> Thierry Brousse,<sup>4,5,\*</sup> Stéphane Lucas,<sup>1</sup> Laurent Houssiau,<sup>6</sup> Jean-Jacques Pireaux,<sup>6</sup> and Amine Achour<sup>6,z</sup>

<sup>1</sup>Laboratoire d'Analyse par Réactions Nucléaires (LARN), Namur Institute of Structured Matter (NISM), University of Namur, Namur, Belgium

<sup>2</sup>Univ. Lille, CNRS, Central Lille, Univ. Polytechnique Hauts-de-France, UMR 8520, IEMN, F-59000 Lille, France

<sup>3</sup>Université de Lorraine, CNRS, IJL, F-54000 Nancy, France

<sup>4</sup>Nantes Université, CNRS, Institut des Matériaux de Nantes Jean Rouxel, IMN, F-44000 Nantes, France

<sup>5</sup>Réseau sur le Stockage Electrochimique de l'Energie (RS2E), CNRS FR 3459, F-80039, Amiens France

<sup>6</sup>Laboratoire Interdisciplinaire de Spectroscopie Electronique (LISE), Namur Institute of Structured Matter (NISM), University of Namur, Namur, Belgium

<sup>z</sup>E-mail: emile.haye@unamur.be; a\_aminph@yahoo.fr

\*Electrochemical Society Member.

## Abstract

In this study, the tuning of the KOH electrolyte composition is proposed as a strategy to drastically limit the capacitance fade of vanadium nitride (VN) electrode. We demonstrate that the use of a  $V^{5+}$  (as  $VO_4^{3-}$  vanadates anions) containing KOH electrolyte enhances the cycling stability of VN thin film electrode : a loss of 59% of

1  
2  
3 the capacitance is observed for the electrode tested in KOH over 3000 consecutive  
4 cycles. After  $V^{5+}$  addition in the electrolyte, the capacitance fade is decreased to 23%.  
5  
6 Furthermore, the presence of  $V^{5+}$  species in the solution leads to VN capacitance  
7 enhancement from  $379 \text{ mF cm}^{-2}$  for  $V^{5+}$  ions free electrolyte up to  $577 \text{ mF cm}^{-2}$  at  $5$   
8  $\text{mV s}^{-1}$  for  $V^{5+}$ -containing KOH solution. The enhanced cycling stability is attributed to  
9 the stabilization of an oxide/oxynitride layer at the VN surface, instead of its  
10 dissolution, thanks to the chemical equilibrium shift of the VN dissolution reaction. This  
11 simple and innovative strategy consisting in tuning the electrolyte composition opens  
12 new pathways for other systems that suffer from electrode dissolution in the electrolyte  
13 while being electrochemically cycled.  
14  
15  
16  
17  
18  
19  
20  
21  
22  
23  
24  
25  
26

## 27 Introduction

28  
29 Recently, vanadium nitride (VN) has been identified as one of the most promising  
30 transition metal compound for use in electrochemical capacitors (ECs) with a specific  
31 capacitance as high as  $1340 \text{ F g}^{-1}$  in a KOH electrolyte solution [1–12]. This  
32 impressive capacitance has been attributed to a combination of both a double layer-  
33 type capacitance and a pseudo-capacitance occurring at this nitride surface [2,6,13].  
34 However, VN suffers from poor cycling stability, which hinders its practical use [14]. In  
35 the related literature, this poor cycling ability has been ascribed to the dissolution and  
36 non-stability of the vanadium oxide layer at the surface region, which is responsible  
37 for the pseudo-capacitive behaviour [2,5]. In order to cure such cycling instability  
38 limitation, Morel *et al.* [8] have proposed to decrease the applied potential window (V)  
39 from  $[-1.2:0\text{V}]$  to  $[-1.0:-0.4\text{V}]$  for VN electrode in KOH electrolyte. Although a cycling  
40 stability over 10.000 cycles has been achieved, this led, however, to an energy density  
41 reduction by a factor of 4 for symmetrical VN devices, due to this narrow potential  
42 window. Recently, the stability enhancement of VN in  $\text{K}_2\text{SO}_4$  electrolyte has been  
43  
44  
45  
46  
47  
48  
49  
50  
51  
52  
53  
54  
55  
56  
57  
58  
59  
60

1  
2  
3 reported [4]. However, the specific capacitance in this neutral electrolyte is almost five  
4 times lower compared to that of the same VN electrode tested in KOH electrolyte [5,6].  
5  
6  
7 Despite the fact that VN is electrochemically unstable in aqueous alkaline electrolytes  
8 including KOH, this type of electrolyte offers the best capacitance performance due to  
9  
10 fast reversible redox reactions, involving surface oxide groups and OH<sup>-</sup> ions from the  
11  
12 electrolyte [2,15]. To the best of our knowledge, only Lu *et al.* [16] have stabilized VN  
13  
14 electrode over a relatively large number of charge/discharge cycles (15000 cycles with  
15  
16 88% retention) in KOH electrolyte by coating VN with an ultra-thin carbon layer, without  
17  
18 sacrificing the capacitance or energy density. In the present study, a new strategy is  
19  
20 proposed to limit the capacitance loss of VN that can complement the previously  
21  
22 reported methods. Indeed, the decline of VN capacitance involves the loss of V<sup>5+</sup>  
23  
24 and/or V<sup>4+</sup> ions by dissolution from the oxide layer at the oxidized surface region of the  
25  
26 VN compound [2,4,5]. We demonstrate that the use of a V<sup>5+</sup>-containing KOH  
27  
28 electrolyte offers a simple, yet effective, strategy to suppress the capacitance loss of  
29  
30 VN. We also report on the effect of the V<sup>5+</sup> species in the electrolyte on the  
31  
32 enhancement of the specific capacitance of the VN electrodes by more than 1.5-fold  
33  
34 compared to the electrolyte without V<sup>5+</sup> species.  
35  
36  
37  
38  
39  
40  
41  
42

### 43 **Materials and methods**

44  
45  
46 VN films were deposited on silicon substrates by reactive magnetron sputtering of a  
47  
48 rectangular vanadium target (330x50x6 mm) in a gas mixture of Ar/N<sub>2</sub> using a semi-  
49  
50 industrial sputtering machine (Vinci Technologies). The target-substrate distance was  
51  
52 5 cm, with a back and forth movement of the substrate in front of the target. The current  
53  
54 applied to the target was fixed to 1.5 A using a pulsed-DC Pinnacle/Advanced Energy  
55  
56 power supply at 50 kHz, with  $t_{\text{OFF}} = 4 \mu\text{s}$ . The Ar and N<sub>2</sub> flow rates were kept at 30 and  
57  
58 5 sccm, respectively, leading to a total gas pressure of 1.1 Pa. No substrate bias was  
59  
60

1  
2  
3 applied during deposition. After deposition, the morphology of the film was investigated  
4  
5 by scanning electron microscopy (SEM), using a JEOL JSM 7500F microscope. The  
6  
7 structure of the deposited films was assessed by X-ray diffraction (XRD)  
8  
9 measurements on a PANalytical X'Pert PRO diffractometer, using Cu K $\alpha$  radiation  
10  
11 (1.5406 Å). The measurement was performed in a  $\theta/\theta$ - $\omega$  configuration, with an offset  
12  
13  $\omega$  angle of 2° avoiding the strong diffraction of the silicon substrate. The chemical  
14  
15 composition of the VN thin film was investigated before and after electrochemical tests  
16  
17 by X-ray photoelectron spectroscopy (XPS), performed on a Thermo Scientific K-  
18  
19 Alpha spectrometer (Al K $\alpha$  at 1486.68 eV, spot size of 250×250  $\mu$ m). No surface  
20  
21 cleaning was performed before the analysis. A flood gun was applied for charge  
22  
23 compensation. XPS depth profiling was used to reveal the chemical changes that  
24  
25 occurred on the surface and the bulk of the material. An Ar<sup>+</sup> beam at 2 keV (raster size  
26  
27 1.25×1.25 mm<sup>2</sup>, 30°, 3.3  $\mu$ A) was used, with a step size of 20 s. The N 1s, O 1s and  
28  
29 V 2p levels were recorded at a pass energy of 50 eV with a single scan. The authors  
30  
31 are aware that ion beam may induce modification of chemical state, especially on  
32  
33 vanadium. In this view, the conclusion is more oriented on element concentration  
34  
35 rather than the changes of chemistry.  
36  
37  
38  
39  
40  
41  
42

43 The electrochemical characterization was performed in a standard three-electrode cell  
44  
45 system, in which VN (1×1 cm<sup>2</sup>), Hg/HgO and platinum plates act respectively as  
46  
47 working, reference and counter electrodes. The electrolyte was prepared by adding  
48  
49 0.05 or 0.1 M V<sub>2</sub>O<sub>5</sub> into a 1 M KOH solution.  
50  
51

52 Cyclic voltammetry (CV) was conducted in a potential window from -0.9 to 0 V (vs.  
53  
54 Hg/HgO) at different scan rates: 5, 10, 20, 50 and 100 mV s<sup>-1</sup>.  
55  
56  
57  
58  
59  
60

According to the Pourbaix diagram of vanadium (Figure 1), the dissolution of  $V_2O_5$  powder in 1M KOH, namely at pH 14, leads to the formation of tetrahedral  $VO_4^{3-}$  vanadates ions, with  $V^{5+}$  oxidation state.

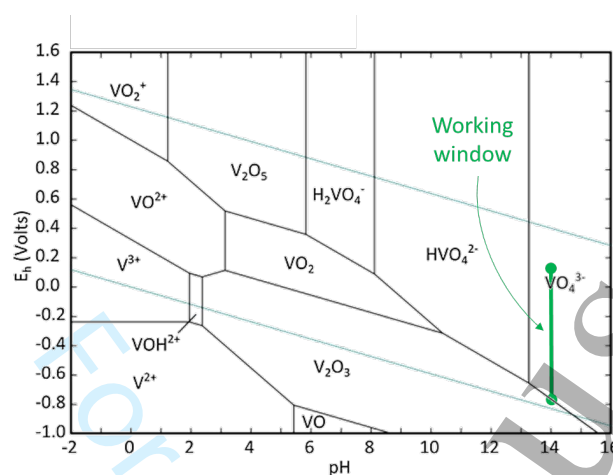


Figure 1. Pourbaix diagram of vanadium oxide with the working window, adapted from [17]

Galvanostatic charge discharge (GCD) measurements were carried out at current densities of 1, 2, 3, 5 and 10  $mA\ cm^{-2}$ , in a potential window from -0.8 to 0 V.

Electrochemical Impedance spectroscopy (EIS) was performed in the frequency range of 100 kHz to 0.01 Hz with a 10 mV ac amplitude.

The average specific capacitance was calculated from the cyclic voltammetry (CV) plots, using the following equation:

$$C_{sq}(mF \cdot cm^{-2}) = \frac{\int I dV}{\Delta V \times \nu}$$

where  $I$  represents the oxidation current density, and  $\Delta V$  is the potential window,  $\nu$  is the scanning rate. For some distorted CVs obtained at fast scan rates, the same equation was used although this is quite difficult to provide a capacitance value in such



1  
2  
3 case, and this was done for comparison purpose only with the values determined at  
4  
5 low scan rates.  
6

7  
8 The average specific capacitance was calculated from the galvanostatic discharge  
9  
10 curves, using the following equation:  
11

$$12 \quad C_{sq}(mF \cdot cm^{-2}) = \frac{I \Delta t}{\Delta V \times A}$$

13  
14  
15  
16  
17  
18 Where  $I$  denotes the current density,  $\Delta t$  is the discharge time, and  $\Delta V$  is the width of  
19  
20 the potential window during discharge,  $A$  is the area of active materials.  
21

22  
23 Faradaic efficiency were calculated from the galvanostatic charge and discharge  
24  
25 curves, using the following equation:  
26

$$27 \quad \text{Faradaic efficiency} = \frac{t(\text{discharge})}{t(\text{charge})} \times 100\%$$

## 28 29 30 31 32 33 34 35 **Results and discussion**

36  
37  
38 The morphology and structure of the VN electrodes are presented in **Figure 2**. From  
39  
40 the top and cross section SEM observations (**Figure 2 a and b**), a homogeneous  
41  
42 columnar microstructure is observed, with cubic crystallites pointing at the surface, in  
43  
44 agreement with previous works on transition metal nitride thin films, deposited without  
45  
46 substrate bias [18,19]. The good crystallinity of the film is confirmed by XRD  
47  
48 measurement (**Figure 2.c**), with an intense peak at  $37.6^\circ$ , attributed to the (111) peak  
49  
50 of cubic VN [20]. Such a strong (111) preferred orientation is typical for transition metal  
51  
52 nitride films deposited without bias. The crystallite size is around 22 nm, as estimated  
53  
54 from the Debye-Scherrer formula, in agreement with SEM observation. The film  
55  
56 thickness determined from the cross-section SEM image is around 550 nm.  
57  
58  
59  
60

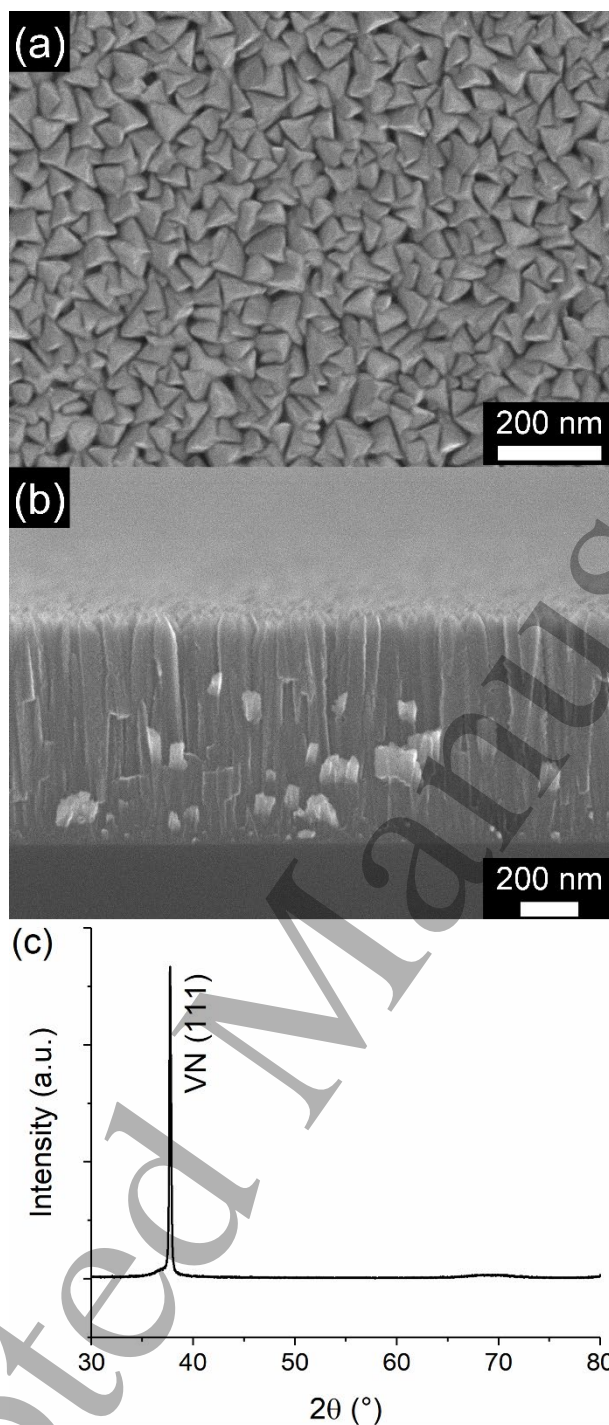


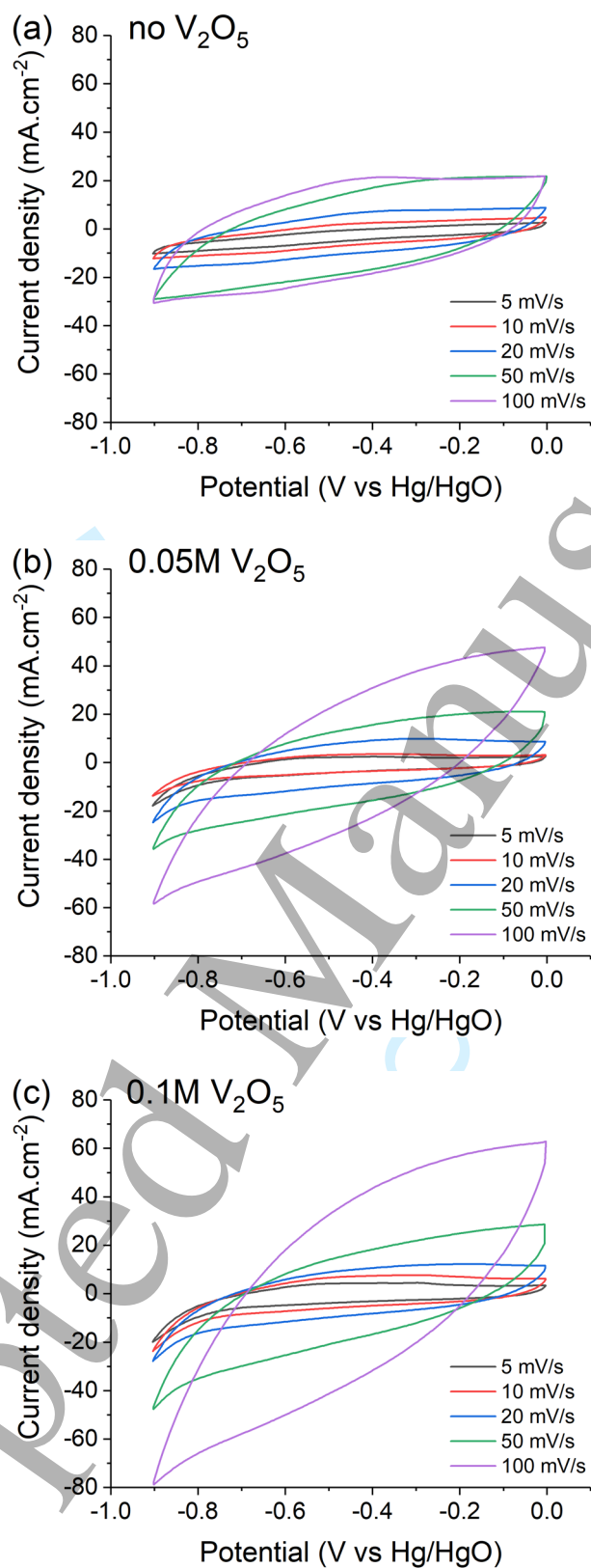
**Figure 2.** (a) top and (b) cross section SEM observations, and (c) XRD pattern of the VN electrode.

The electrochemical behavior of the VN electrodes were assessed in 1 M KOH aqueous solution with or without the addition of  $V_2O_5$  in a usual 3-electrode cell. The cyclic voltammograms (CV) of the VN film in 1 M KOH, 1 M KOH + 0.05 M  $V_2O_5$  and 1 M KOH + 0.1 M  $V_2O_5$  as a function of scan rate in the potential range of -0.9 to 0 V

1  
2  
3 are presented in **Figure 3**. The VN films show a pseudocapacitive behaviour under all  
4 tested conditions. Obviously, the specific capacitance of the VN electrode in 1 M KOH  
5 aqueous solution decreases from 379 to 154 mF cm<sup>-2</sup> (Table 1, **Figure 4**) upon  
6 increasing the scan rate from 5 to 100 mV s<sup>-1</sup>, while the shape of the CVs remains  
7 almost unaltered, suggesting that the electrode owns a good rate capability. Distortion  
8 is noted at high scan rate, indicating the loss of capacitive behaviour, but the specific  
9 capacitance is still given for comparative purpose.

10  
11  
12 A low potential (between -0.9 and -0.8 V vs Hg/HgO), a slight current density variation  
13 is observed, due to some reduction of VO<sub>4</sub><sup>3-</sup> (with V<sup>5+</sup>) into V<sub>2</sub>O<sub>3</sub> (with V<sup>3+</sup>), in  
14 accordance with the Pourbaix diagram (Figure 1).

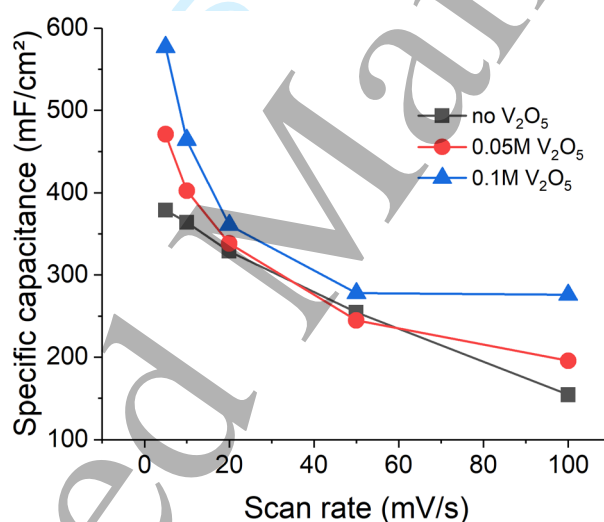
15  
16  
17 Addition of V<sub>2</sub>O<sub>5</sub> in the electrolyte promotes a significant increase of the specific  
18 capacitance (Cs) for all investigated scan rates under our experimental conditions,  
19 although a slight distortion of the CVs was observed. Indeed, addition of V<sub>2</sub>O<sub>5</sub> in the  
20 electrolytic solution (1 M KOH) led to an increase of the specific capacitance from 379  
21 mF cm<sup>-2</sup> (1 M KOH) to 471 mF cm<sup>-2</sup> (1 M KOH + 0.05 M V<sub>2</sub>O<sub>5</sub>) and 577 mF cm<sup>-2</sup> (1 M  
22 KOH + 0.1 M V<sub>2</sub>O<sub>5</sub>) at a sweep rate of 5 mV s<sup>-1</sup>. This behaviour is most likely due to  
23 reduced effective interaction between the electrode surface and OH<sup>-</sup> anions at higher  
24 scan rates.  
25  
26  
27  
28  
29  
30  
31  
32  
33  
34  
35  
36  
37  
38  
39  
40  
41  
42  
43  
44  
45  
46  
47  
48  
49  
50  
51  
52  
53  
54  
55  
56  
57  
58  
59  
60



**Figure 3.** Cyclic voltammetric curves of VN electrodes in (a) 1 M KOH, (b) 1 M KOH + 0.05M V<sub>2</sub>O<sub>5</sub> and (c) 1 M KOH + 0.1 M V<sub>2</sub>O<sub>5</sub> at scan rates of 5, 10, 20, 50 and 100 mV s<sup>-1</sup>

**Table 1.** The values of the specific capacitance  $C_s$  versus scan rate of the VN electrodes in KOH without and with, 0.05M, and 0.1 M  $V_2O_5$ 

Scan rate ( $mV s^{-1}$ )	$C_s$ ( $mF cm^{-2}$ ) in 1 M KOH	$C_s$ ( $mF cm^{-2}$ ) in 1 M KOH + 0.05M $V_2O_5$	$C_s$ ( $mF cm^{-2}$ ) in 1 M KOH + 0.1 M $V_2O_5$
5	379	471	577
10	364	402	464
20	329	338	361
50	254	245	278
100	154	196	276

**Figure 4.** Evolution of the specific capacitance of VN at different scan rates in different KOH electrolytes.

The corresponding galvanostatic charge-discharge plots at a current densities of 1, 2, 3, 5 and 10  $mA/cm^2$  in the -0.8 to 0 V range are shown in **Figure 5** while the calculated specific capacitance values are summarized in Table 2. No significant IR drop was reported, as in the case of CrN [21], indicating a better conductivity. A similar trend –

1  
2  
3 i.e. a decrease of the specific capacitance values – was evidenced in all systems upon  
4 increasing the current density. Generally, the retention of the specific capacitance with  
5 current density depends on: i) diffusion of ions in electrolyte, ii) adsorption of ions on  
6 the electrode surface, and iii) charge transfer between electrode and electrolyte.  
7  
8 Enhancing the current density could slow any of the above-mentioned conditions,  
9  
10 leading to the decrease of the specific capacitance.  
11  
12  
13  
14  
15  
16  
17  
18  
19  
20  
21  
22  
23  
24  
25  
26  
27  
28  
29  
30  
31  
32  
33  
34  
35  
36  
37  
38  
39  
40  
41  
42  
43  
44  
45  
46  
47  
48  
49  
50  
51  
52  
53  
54  
55  
56  
57  
58  
59  
60

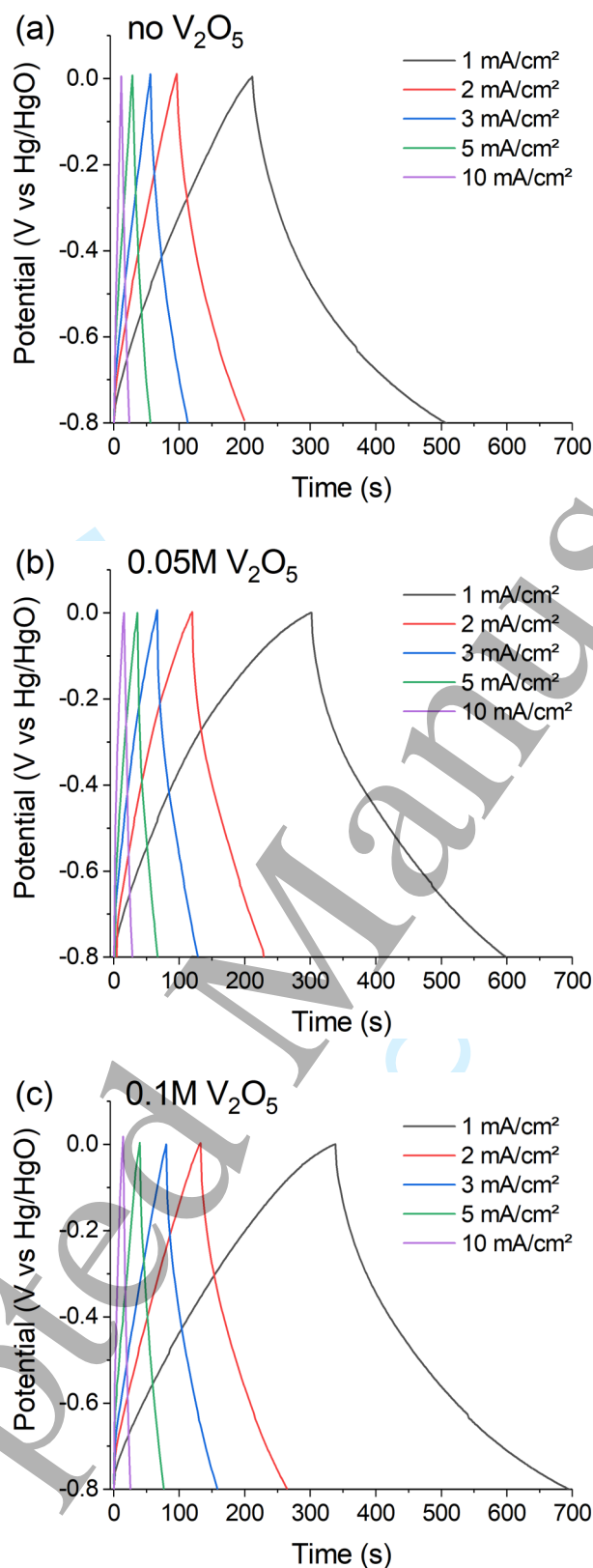


**Figure 5.** Galvanostatic charge discharge curves of VN electrodes in (a) 1 M KOH, (b) 1 M KOH + 0.05M  $V_2O_5$  and (c) 1 M KOH + 0.1 M  $V_2O_5$  at current densities of 1, 2, 3, 5 and 10  $mA \cdot cm^{-2}$ .



**Table 2.** The values of  $C_s$  as a function of current density of the VN electrodes in 1 M KOH without and with 0.05M, and 0.1 M of  $V_2O_5$ .

Current density (mA/cm <sup>2</sup> )	$C_s$ (mF cm <sup>-2</sup> ) in 1 M KOH	$C_s$ (mF cm <sup>-2</sup> ) In 1 M KOH + 0.05M $V_2O_5$	$C_s$ (mF cm <sup>-2</sup> ) in 1 M KOH + 0.1 M $V_2O_5$
1	373	371	456
2	260	273	330
3	218	236	300
5	177	194	231
10	150	169	153

In order to gain a better understanding on the electrochemical behaviour of the electrode/electrolyte interface during the charge storage process, electrochemical impedance spectroscopy (EIS) measurements were performed in the frequency range from 100 kHz to 0.01 Hz in 1 M KOH (**Figure 6**). The equivalent Randles circuit of the Nyquist plot is shown in the inset of Figure 5 and includes a solution resistance ( $R_s$ ), constant phase element (CPE), charge transfer resistance ( $R_{ct}$ ) and Warburg element ( $W$ ), with values presented in Table 3. The EIS analysis revealed that the Nyquist plots are similar in shape and exhibit a small semicircle at high frequency region and a slope line (Warburg curve) in the low frequency region.

The low resistance values in the 1 M KOH + 0.1 M  $V_2O_5$  electrolyte correlate with enhanced conductivity of the VN electrode when  $V_2O_5$  is dissolved in the electrolytic solution to provide  $VO_4^{3-}$  vanadates ions.



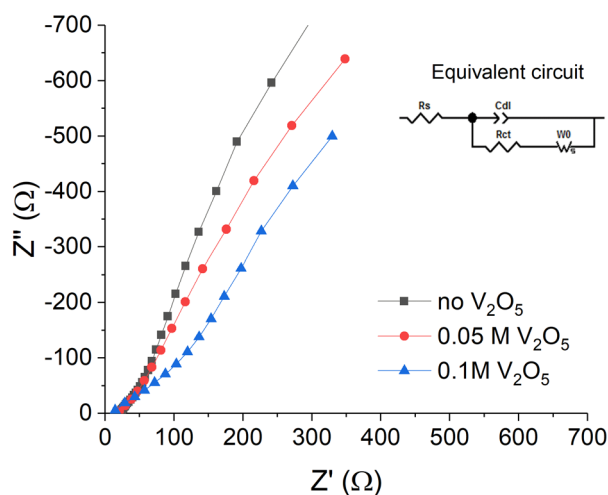


**Figure 6.** Electrochemical Impedance spectroscopy (EIS) measurements of the VN electrodes in different KOH electrolytes and their EIS equivalent circuit in 1 M KOH aqueous solution without and with 0.05M, and 0.1 M  $V_2O_5$

**Table 3.**  $R_{ct}$  and  $R_s$  values of VN electrodes in 1 M KOH without and with 0.05M, and 0.1 M  $V_2O_5$

EIS	$R_s$ ( $\Omega$ )	$R_{ct}$ ( $\Omega$ )
VN in bare 1KOH	17.12	260
VN in 1 M KOH with 0.05M $V_2O_5$	17.45	240.3
VN in 1 M KOH with 0.1 M $V_2O_5$	17.25	140.7

Finally, the cycling stability of the VN electrodes was investigated in the different electrolytic solutions, namely, 1 M KOH, 1 M KOH+0.05 M  $V_2O_5$  and KOH+0.1 M  $V_2O_5$  in the potential window of -0.9 to 0V at a scan rate of  $50 \text{ mV s}^{-1}$  (**Figure 6**). All the capacitance values experienced a continuous decrease for the first 1600 cycles then remained almost unaffected up to 3000 cycles. The most important feature of this figure is the highest retention (77%) of the initial capacitance recorded for the VN

electrode in 1 M KOH + 0.1 M V<sub>2</sub>O<sub>5</sub>, as compared to retention of 60% and 41% achieved in the 1 M KOH + 0.05 M V<sub>2</sub>O<sub>5</sub> and 1 M KOH solutions, respectively (Table 4). Again, these results again evidence the improvement of the energy storage performance and stability of the VN electrode by simply altering the composition of the electrolytic solution through the addition of vanadates ions.

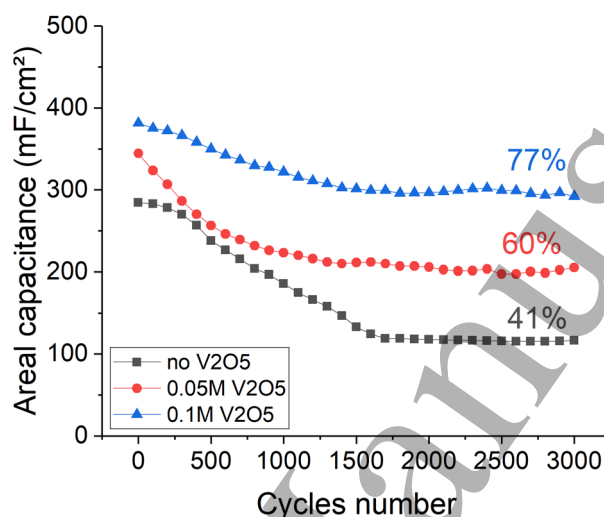


**Figure 6.** Evolution of the areal capacitance vs. the number of cycles of the VN electrode in the different KOH electrolytes for 3000 cycles (potential window:  $-0.9$  to  $0\text{V}$  (vs. Hg/HgO), scanning rate:  $50\text{ mV s}^{-1}$ ).

**Table 4.** Cycling stability of the VN electrodes in 1 M KOH without and with 0.05 M, and 0.1 M V<sub>2</sub>O<sub>5</sub>

Electrolyte	Cs initial (mF cm <sup>-2</sup> )	Cs after 3000 cycles (mF cm <sup>-2</sup> )	Cs retention (%)
1 M KOH	284	117	41
1 M KOH + 0.05M V <sub>2</sub> O <sub>5</sub>	345	205	60
1 M KOH + 0.1 M V <sub>2</sub> O <sub>5</sub>	381	292	77

1  
2  
3 To investigate the origin of the modification of the charge storage by adding  $V_2O_5$  in 1  
4 M KOH electrolyte, XPS analyses were performed on the VN electrodes before and  
5 after cycling. The electrodes were etched using argon plasma to record depth profiles  
6 during 350s, corresponding to a depth of 100 nm. It is important to remember that the  
7 film presents a porous columnar microstructure, as shown on the SEM observation  
8 (**Figure 2**). **Figure 7** depicts the O 1s and V 2p core levels spectra within the coating  
9 (etching time 350s) and on the surface (etching time 20s) for VN film after deposition  
10 and after cycling in 1 M KOH, 1 M KOH+0.05 M  $V_2O_5$  and KOH+0.1 M  $V_2O_5$ . The very  
11 first spectra are not presented as the signal heavily depends on surface contamination,  
12 especially after electrochemical tests. Although it is delicate to identify the chemical  
13 state of vanadium because of potential ion beam induced damages, it is clear that the  
14 bulk (Figure 7.a) and the surface (Figure 7.b) contain more oxygen (and thus more  
15 oxidized species) when the electrodes are cycled in KOH containing  $V_2O_5$ .  
16  
17  
18  
19  
20  
21  
22  
23  
24  
25  
26  
27  
28  
29  
30  
31  
32  
33  
34  
35  
36  
37  
38  
39  
40  
41  
42  
43  
44  
45  
46  
47  
48  
49  
50  
51  
52  
53  
54  
55  
56  
57  
58  
59  
60

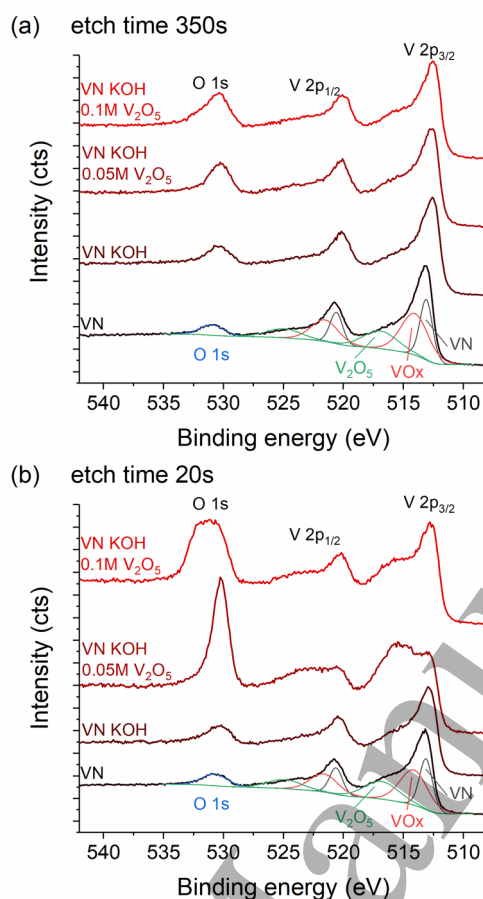


Figure 7. O 1s and V 2p core level spectra of VN electrodes before and after cycling in the different KOH electrolytes, (a) in the bulk (etching time 350s) and (b) at the surface (etching time 20s)

The entire XPS depth profiles (Figure S1) and the concentration evolutions of O 1s and V 2p contributions (Figure S2) are given in the supplementary information. One can note that the as-deposited VN electrode is nearly stoichiometric, with a nitrogen concentration of  $\approx 40\%$  vanadium content of  $\approx 50\%$ , and an oxygen content of  $\approx 10\%$ . Such oxygen content is often observed in TMN nitride deposited by PVD [18]. The oxygen content within the coating (signal averaged from 100 to 300s of the profile) increases to about 16, 25 and 28 at.% after cycling in 1 M KOH, 1 M KOH + 0.05 M V<sub>2</sub>O<sub>5</sub> and 1 M KOH + 0.1 M V<sub>2</sub>O<sub>5</sub>, respectively. At the same time, the nitrogen content decreases from 40 to 28% for 1 M KOH + 0.1 M V<sub>2</sub>O<sub>5</sub> electrolyte. Concerning the signal

1  
2  
3 of vanadium, the two oxide peaks at  $514.0\pm 0.1$  and  $517.0\pm 0.1$  eV, respectively  
4 attributed to  $\text{VO}_x$  (with  $x\approx 2$ ) and  $\text{V}_2\text{O}_5$  are more intense at the surface, when cycled in  
5  
6 the  $\text{V}_2\text{O}_5$ -containing electrolyte.  
7  
8  
9

10 The understanding of surface mechanisms when the VN electrode is cycled in  $\text{V}_2\text{O}_5$ -  
11 containing electrolyte is not obvious. First, the dissolution of  $\text{V}_2\text{O}_5$  leads to the  
12 presence of vanadates  $\text{VO}_4^{3-}$  ions, with  $\text{V}^{5+}$  oxidation state, according to Pourbaix  
13 diagram (Figure 1). However, during the cycling, an equilibrium between  $\text{V}^{3+}$  from the  
14 electrode surface and  $\text{V}^{5+}$  from the electrolyte is established on the electrode surface,  
15 which is out of the thermodynamic equilibrium. These redox reactions are randomly  
16 occurring at the surface of the electrode which explains the distribution of potential  
17 observed from the CVs, which is typically observed for pseudocapacitive  
18 electrodes[22,23]. It does not seem that preferential sites are involved since the redox  
19 reactions do not translate in a well-defined pair of redox peaks on the CVs.  
20  
21  
22  
23  
24  
25  
26  
27  
28  
29  
30  
31  
32  
33

34 In the working conditions, VN (where V oxidation state is +3) tends to dissolve into the  
35 KOH electrolyte to form  $\text{VO}_4^{3-}$  ions (with  $\text{V}^{5+}$  oxidation state), as it is the most stable  
36 specie according to the Pourbaix diagram. This dissolution probably occurs in two  
37 subsequent steps, with first surface oxidation of VN, followed by the oxide dissolution.  
38 This assumption is supported by the slight increase of oxygen content when  
39 comparing XPS depth profiles of as deposited VN and VN cycled in 1M KOH without  
40  $\text{V}_2\text{O}_5$  (Figure S1.a and b). Each of these steps are characterized by a rate constant  
41 and an equilibrium. The presence of vanadates ions in the electrolyte shift the  
42 equilibrium of surface oxide dissolution according to Le Chatelier principle. Then, the  
43 previous step, namely reversible surface oxidation, becomes predominant, and the  
44 oxide dissolution no longer occurs, resulting in the formation of thick surface oxide, as  
45 observed in XPS.  
46  
47  
48  
49  
50  
51  
52  
53  
54  
55  
56  
57  
58  
59  
60

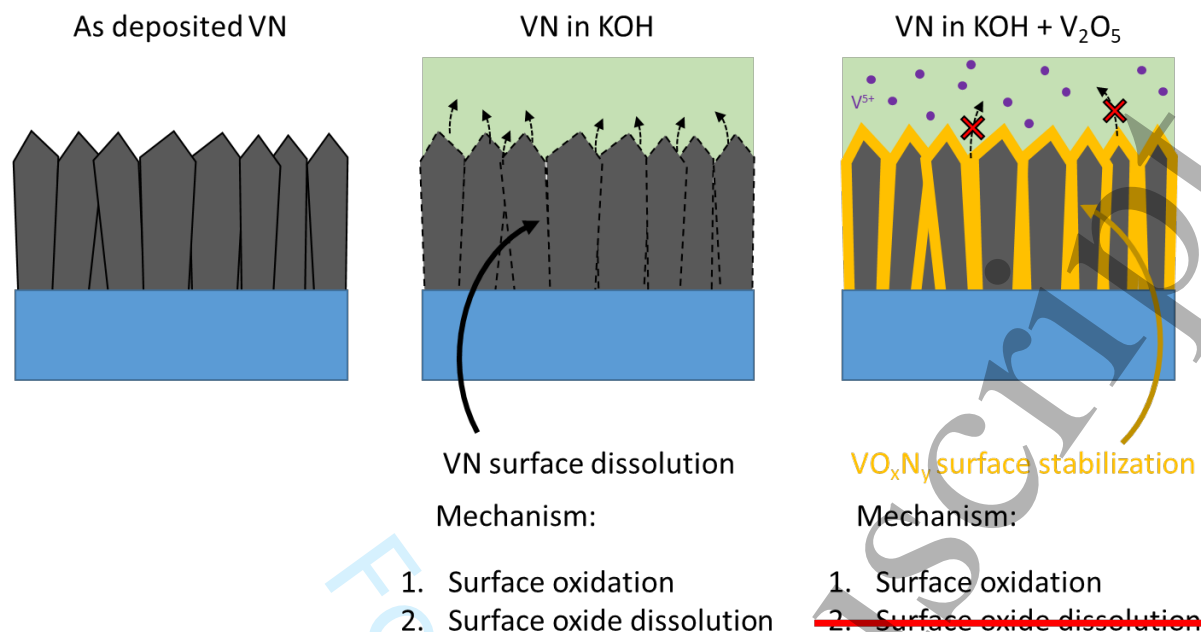


**Figure 8.** Sketch of surface evolution of VN film in different electrolytes. The thick yellow line corresponds to the stabilization of the oxide/oxy-nitride layer.

The **Figure 8** summarizes the surface evolution of VN, depending the electrolyte, with the stabilization of oxide/oxy-nitride layer. As the coating is highly porous, with columnar morphology, the formation of oxide occurs all along the column surface, resulting in the observation of high oxygen content even at high erosion time during XPS analysis. The distortion of the CV curves (**Figure 3**) in the presence of V<sub>2</sub>O<sub>5</sub> also corroborates the higher resistivity of the oxide layer compared to VN.

## Conclusion

In the present work, a new strategy is proposed to improve the cycling stability of vanadium nitride thin film in KOH, by adding V<sup>5+</sup> ions in the electrolyte, introduced as VO<sub>4</sub><sup>3-</sup> vanadate anions. According to Le Chatelier principles, the chemical equilibrium of the VN dissolution reaction is shifted, leading to the stabilization of an oxide/oxy-nitride layer at the VN surface. While the capacitance drops by 59% for VN

1  
2  
3 in 1 M KOH, the drop can be limited to 23% in 1 M KOH + 0.1 M V<sub>2</sub>O<sub>5</sub>. Furthermore,  
4  
5 a capacitance increase by the VN electrodes by more than 1.5 fold was observed upon  
6  
7 V<sup>5+</sup> saturation, although, a slight distortion of the CV curve was also noticed, may be  
8  
9 due to the presence of more resistive oxide on VN surface. This simple and innovative  
10  
11 strategy can be implemented for other systems that suffer from dissolution in the  
12  
13 electrolytic solution.  
14  
15

### 16 17 **Acknowledgments**

18  
19  
20 The authors thank the Synthesis, Irradiation & Analysis of Materials (SIAM), Morph'IM  
21  
22 and PC<sup>2</sup> platforms of the University of Namur for XPS, SEM and XRD measurements.  
23  
24 E.H., S.L. D.P. and J.F.P. acknowledge Wallonia Brussel International and Campus  
25  
26 France for funding the PLASMOCAPS project, done in the framework of Belgo-French  
27  
28 Project HUBERT CURIEN TOURNESOL. TB and CD acknowledge LABEX STORE-  
29  
30 EX (ANR 10-LABX-0076) for financial support.  
31  
32  
33  
34  
35  
36  
37  
38  
39  
40  
41  
42  
43  
44  
45  
46  
47  
48  
49  
50  
51  
52  
53  
54  
55  
56  
57  
58  
59  
60



## References

- [1] R. Lucio-Porto, S. Bouhtiyya, J.F. Pierson, A. Morel, F. Capon, P. Boulet, T. Brousse, VN thin films as electrode materials for electrochemical capacitors, *Electrochimica Acta*. 141 (2014) 203–211. <https://doi.org/10.1016/j.electacta.2014.07.056>.
- [2] D. Choi, G.E. Blomgren, P.N. Kumta, Fast and Reversible Surface Redox Reaction in Nanocrystalline Vanadium Nitride Supercapacitors, *Adv. Mater.* 18 (2006) 1178–1182. <https://doi.org/10.1002/adma.200502471>.
- [3] A. Djire, P. Pande, A. Deb, J.B. Siegel, O.T. Ajenifujah, L. He, A.E. Sleightholme, P.G. Rasmussen, L.T. Thompson, Unveiling the pseudocapacitive charge storage mechanisms of nanostructured vanadium nitrides using in-situ analyses, *Nano Energy*. 60 (2019) 72–81. <https://doi.org/10.1016/j.nanoen.2019.03.003>.
- [4] A. Achour, M. Islam, I. Ahmad, K. Saeed, S. Solaymani, Electrochemical Stability Enhancement in Reactive Magnetron Sputtered VN Films upon Annealing Treatment, *Coatings*. 9 (2019) 72. <https://doi.org/10.3390/coatings9020072>.
- [5] N. Ouldhamadouche, A. Achour, R. Lucio-Porto, M. Islam, S. Solaymani, A. Arman, A. Ahmadpourian, H. Achour, L. Le Brizoual, M.A. Djouadi, T. Brousse, Electrodes based on nano-tree-like vanadium nitride and carbon nanotubes for micro-supercapacitors, *J Mater Sci Technol.* 34 (2018) 976–982. <https://doi.org/10.1016/j.jmst.2017.11.048>.
- [6] A. Achour, R. Lucio-Porto, S. Solaymani, M. Islam, I. Ahmad, T. Brousse, Reactive sputtering of vanadium nitride thin films as pseudo-capacitor electrodes for high areal capacitance and cyclic stability, *J Mater Sci: Mater Electron.* 29 (2018) 13125–13131. <https://doi.org/10.1007/s10854-018-9435-z>.
- [7] P.J. Hanumantha, M.K. Datta, K.S. Kadakia, D.H. Hong, S.J. Chung, M.C. Tam, J.A. Poston, A. Manivannan, P.N. Kumta, A Simple Low Temperature Synthesis of Nanostructured Vanadium Nitride for Supercapacitor Applications, *J. Electrochem. Soc.* 160 (2013) A2195. <https://doi.org/10.1149/2.081311jes>.
- [8] A. Morel, Y. Borjon-Piron, R.L. Porto, T. Brousse, D. Bélanger, Suitable Conditions for the Use of Vanadium Nitride as an Electrode for Electrochemical Capacitor, *J. Electrochem. Soc.* 163 (2016) A1077. <https://doi.org/10.1149/2.1221606jes>.
- [9] P.J. Hanumantha, M.K. Datta, K. Kadakia, C. Okoli, P. Patel, P.N. Kumta, Vanadium nitride supercapacitors: Effect of Processing Parameters on electrochemical charge storage behavior, *Electrochimica Acta*. 207 (2016) 37–47. <https://doi.org/10.1016/j.electacta.2016.04.058>.
- [10] B. Gao, X. Li, X. Guo, X. Zhang, X. Peng, L. Wang, J. Fu, P.K. Chu, K. Huo, Nitrogen-Doped Carbon Encapsulated Mesoporous Vanadium Nitride Nanowires as Self-Supported Electrodes for Flexible All-Solid-State Supercapacitors, *Advanced Materials Interfaces*. 2 (2015) 1500211. <https://doi.org/10.1002/admi.201500211>.
- [11] Q. Li, Y. Chen, J. Zhang, W. Tian, L. Wang, Z. Ren, X. Ren, X. Li, B. Gao, X. Peng, P.K. Chu, K. Huo, Spatially confined synthesis of vanadium nitride nanodots intercalated carbon nanosheets with ultrahigh volumetric capacitance and long life for flexible supercapacitors, *Nano Energy*. 51 (2018) 128–136. <https://doi.org/10.1016/j.nanoen.2018.06.053>.
- [12] X. Xiao, X. Peng, H. Jin, T. Li, C. Zhang, B. Gao, B. Hu, K. Huo, J. Zhou, Freestanding Mesoporous VN/CNT Hybrid Electrodes for Flexible All-Solid-State



- Supercapacitors, *Adv. Mater.* 25 (2013) 5091–5097.  
<https://doi.org/10.1002/adma.201301465>.
- [13] O. Bondarchuk, A. Morel, D. Bélanger, E. Goikolea, T. Brousse, R. Mysyk, Thin films of pure vanadium nitride: Evidence for anomalous non-faradaic capacitance, *Journal of Power Sources*. 324 (2016) 439–446.  
<https://doi.org/10.1016/j.jpowsour.2016.05.093>.
- [14] K. Robert, C. Douard, A. Demortière, F. Blanchard, P. Roussel, T. Brousse, C. Lethien, On Chip Interdigitated Micro-Supercapacitors Based on Sputtered Bifunctional Vanadium Nitride Thin Films with Finely Tuned Inter- and Intracolumnar Porosities, *Adv. Mater. Technol.* 3 (2018) 1800036.  
<https://doi.org/10.1002/admt.201800036>.
- [15] K. Robert, D. Stiévenard, D. Deresmes, C. Douard, A. Iadecola, D. Troadec, P. Simon, N. Nuns, M. Marinova, M. Huvé, P. Roussel, T. Brousse, C. Lethien, Novel insights into the charge storage mechanism in pseudocapacitive vanadium nitride thick films for high-performance on-chip micro-supercapacitors, *Energy Environ. Sci.* 13 (2020) 949–957. <https://doi.org/10.1039/C9EE03787J>.
- [16] X. Lu, T. Liu, T. Zhai, G. Wang, M. Yu, S. Xie, Y. Ling, C. Liang, Y. Tong, Y. Li, Improving the Cycling Stability of Metal–Nitride Supercapacitor Electrodes with a Thin Carbon Shell, *Advanced Energy Materials*. 4 (2014) 1300994.  
<https://doi.org/10.1002/aenm.201300994>.
- [17] R. Gilligan, A.N. Nikoloski, The extraction of vanadium from titanomagnetites and other sources, *Minerals Engineering*. 146 (2020) 106106.  
<https://doi.org/10.1016/j.mineng.2019.106106>.
- [18] L. Rassinfosse, J.L. Colaux, D. Pilloud, A. Nominé, N. Tumanov, S. Lucas, J.-J. Pireaux, E. Haye, Using ammonia for reactive magnetron sputtering, a possible alternative to HiPIMS?, *Appl. Surf. Sci.* 502 (2020) 144176.  
<https://doi.org/10.1016/j.apsusc.2019.144176>.
- [19] E. Haye, J.L. Colaux, P. Moskovkin, J.-J. Pireaux, S. Lucas, Wide range investigation of duty cycle and frequency effects on bipolar magnetron sputtering of chromium nitride, *Surf. Coat. Technol.* 350 (2018) 84–94.  
<https://doi.org/10.1016/j.surfcoat.2018.07.009>.
- [20] A. Achour, R. Lucio-Porto, M. Chaker, A. Arman, A. Ahmadpourian, M.A. Soussou, M. Boujtita, L. Le Brizoual, M.A. Djouadi, T. Brousse, Titanium vanadium nitride electrode for micro-supercapacitors, *Electrochemistry Communications*. 77 (2017) 40–43.  
<https://doi.org/10.1016/j.elecom.2017.02.011>.
- [21] E. Haye, A. Achour, A. Guerra, F. Moulai, T. Hadjersi, R. Boukherroub, A. Panepinto, T. Brousse, J.-J. Pireaux, S. Lucas, Achieving on chip micro-supercapacitors based on CrN deposited by bipolar magnetron sputtering at glancing angle, *Electrochim. Acta*. 324 (2019) 134890.  
<https://doi.org/10.1016/j.electacta.2019.134890>.
- [22] T. Brousse, D. Bélanger, J.W. Long, To Be or Not To Be Pseudocapacitive?, *J. Electrochem. Soc.* 162 (2015) A5185–A5189.  
<https://doi.org/10.1149/2.0201505jes>.
- [23] P. Simon, Y. Gogotsi, B. Dunn, Where Do Batteries End and Supercapacitors Begin?, *Science*. 343 (2014) 1210–1211.  
<https://doi.org/10.1126/science.1249625>.